

Discrete vs. continuous time implementation of a ring car following model in which overtaking is allowed

S. Jamison, M. McCartney*

School of Computing & Mathematics, University of Ulster, Newtownabbey, BT37 0QB, Northern Ireland, United Kingdom

Received 29 May 2007; accepted 3 October 2007

Abstract

Car following models seek to describe the interactions between individual vehicles as they move along a stretch of road where the behaviour of each vehicle is dependent on the motion of the vehicle directly in front and overtaking is typically not permitted. In this work we study a modified version of the traditional car following model in which the vehicles are travelling on a closed loop and the ‘no overtaking’ restriction has been removed. The resulting model is described firstly in terms of a set of coupled continuous time delay differential equations and then in terms of their discrete time equivalents and both forms of the model are then solved numerically to analyse their post transient behaviour under a periodic perturbation. For certain parameter choices both the continuous and discrete forms of the model can exhibit chaotic behaviour but a comparison of the behaviour of the two models over a wide range of parameter values shows that the discretization can dramatically affect the type of post transient behaviour exhibited. This becomes increasingly evident as the time step used in the discrete time model is increased.

© 2007 Elsevier Ltd. All rights reserved.

Keywords: Car following; Overtaking; Grassberger–Procaccia dimension

1. Introduction

Car following models seek to simulate the motion of an isolated group of individual vehicles on section of road, and they describe how each vehicle in the stream responds to a change in the relative motion of the vehicle ahead by accelerating or braking in a prescribed manner.

Traditionally the properties of car following models have been studied by concentrating on the analysis of traffic behaviour on a single lane stretch of road on which overtaking is not permitted (an overview of which is given by [1, 2]), much recent work however has instead investigated the properties of vehicles moving on a closed circuit or loop (see for example [3–11]).

The work described here is based on a modified and discretized form of the earliest class of car following models which were introduced by Gazis, Herman and Rothery in the early 1960s [12] and are described by

$$\frac{d^2 x_i(t)}{dt^2} = \lambda \frac{\left(\frac{dx_i(t)}{dt} \right)^m \left(\frac{dx_{i-1}(t-\tau)}{dt} - \frac{dx_i(t-\tau)}{dt} \right)}{(x_{i-1}(t-\tau) - x_i(t-\tau))^l} \quad (1)$$

* Corresponding author.

E-mail address: m.mccartney@ulster.ac.uk (M. McCartney).

where $x_i(t)$ is the position of the i th vehicle at time t , λ is a positive constant of proportionality, m and l are positive constants (usually chosen to be integers) and τ is the time it takes a driver (and vehicle) to respond to observed changes in relative velocity and position with respect to the vehicle in front. This class of model is still the subject of significant interest, and in particular with regard to the current work, the presence of chaotic behaviour in (1) has been sought without success [13]. However the addition to (1) of a nonlinear inter-vehicle spacing term has been found to give rise to chaotic motion [14,15].

Car following models are used to simulate the motion of highway traffic and the models used in these simulations are often solved in discrete rather than continuous time in order to decrease computation time (see for example, the Gipps model [16] which forms among others the basis of the UK Transport Research Laboratory's traffic simulation package [17]). In this paper we present a case study illustrating how the method of solution affects the dynamics of the system and the type of behaviour exhibited.

2. The overtaking model

In the current work we consider a discretised linear form of (1) where $m = l = 0$ which represents the motion of n vehicles on a closed loop. In car following models of the form (1), typically the lead vehicle is given some velocity profile, $u_0(t)$ and the resultant motion of the following vehicles is investigated. In a looped model however there is no lead vehicle as it is itself following the last vehicle in the stream, so we give the first ($i = 0$) vehicle in the system a preferred velocity profile, $w_0(t)$. Thus he now updates his behaviour in proportion to the difference between the velocity of his vehicle and the vehicle in front and to the difference between his current and preferred velocities.

This model can be represented as

$$\begin{aligned} \frac{d^2 x_0(t)}{dt^2} &= \lambda \left[\frac{dx_{n-1}(t-\tau)}{dt} - \frac{dx_0(t-\tau)}{dt} \right] + \alpha \left[w_0(t-\tau) - \frac{dx_0(t-\tau)}{dt} \right] \\ \frac{d^2 x_i(t)}{dt^2} &= \lambda \left[\frac{dx_{i-1}(t-\tau)}{dt} - \frac{dx_i(t-\tau)}{dt} \right] \quad \forall i = 1, \dots, n-1. \end{aligned} \quad (2)$$

In the model described by (2) the vehicles are all travelling on a closed circuit of some finite length L and as is typical in car following models, scenarios will occur in which the position of two vehicles can become identical. Such an occurrence would normally be treated as a collision with the simulation being stopped and any subsequent motion being ignored. In this new model however, we treat this type of behaviour as an overtaking manoeuvre and allow the simulation to continue after the governing equations have been re-coupled in accordance with the new order of the vehicles.

We can incorporate overtaking by writing (2) in matrix form as

$$\ddot{\underline{x}}(t) = (\Lambda^\lambda(\underline{x}(t-\tau)) + M^\alpha) \dot{\underline{x}}(t-\tau) + \alpha \begin{bmatrix} w_0(t-\tau) \\ 0 \\ \vdots \\ 0 \end{bmatrix} \quad (3)$$

to explicitly show the dependence of the λ 's on the order of the vehicles in the system at time t . In the above equation \underline{x} is the vector of positions of vehicles on the ring and $\Lambda^\lambda(\underline{x}(t))$ and M^α are square matrices such that

$$M^\alpha = \begin{bmatrix} -\alpha & 0 & \dots & 0 \\ 0 & 0 & \ddots & \vdots \\ \vdots & \ddots & \ddots & \vdots \\ 0 & \dots & \dots & 0 \end{bmatrix} \quad (4)$$

and $\Lambda^\lambda(\underline{x}(t))$ has elements which 'swap' depending on who is following who. Before any overtakings have occurred $\Lambda^\lambda(\underline{x}(t))$ is represented by

$$A^\lambda(\underline{x}(t)) = \begin{bmatrix} -\lambda & 0 & 0 & \cdots & \lambda \\ \lambda & -\lambda & 0 & \cdots & 0 \\ 0 & \lambda & -\lambda & \ddots & 0 \\ \vdots & \ddots & \ddots & \ddots & \vdots \\ 0 & 0 & 0 & \lambda & -\lambda \end{bmatrix}. \quad (5)$$

When the i th vehicle overtakes the vehicle directly in front, the ordering of the vehicles in the stream changes and the resulting change in system structure can be represented in matrix form by interchanging the rows in $A^\lambda(\underline{x}(t))$ corresponding to the vehicles involved in the overtaking manoeuvre followed by the corresponding columns. Thus, for example if vehicle 1 has overtaken vehicle 0 then $A^\lambda(\underline{x}(t))$ is now represented by

$$A^\lambda(\underline{x}(t)) = \begin{bmatrix} -\lambda & \lambda & 0 & \cdots & 0 \\ 0 & -\lambda & 0 & \cdots & \lambda \\ \lambda & 0 & -\lambda & \ddots & 0 \\ \vdots & \ddots & \ddots & \ddots & \vdots \\ 0 & 0 & 0 & \lambda & -\lambda \end{bmatrix}. \quad (6)$$

Investigating [18,19] the behaviour of (3) under periodic perturbation of the form

$$w_0(t) = U_0(1 + A \sin(\omega t)) \quad (7)$$

shows that this overtaking model can give rise to rich chaotic post-transient behaviour. Before examining the behaviour of this model, and its discrete time variant in detail we convert the model into a system with a reduced number of free parameters by writing $\dot{\underline{y}}(t) = \dot{\underline{x}}(t) - \underline{U}_0$ and scaling time as $T = \omega t$ and $\tau_s = \omega \tau$. Setting $\underline{y}(T) = \beta \underline{x}(T)$ and choosing $\beta = \frac{U_0 A}{\omega}$ leads to (3) with $w_0(t)$ of the form (7) now being given by

$$\ddot{\underline{x}}(T) = \left(A^b(\underline{x}(T - \tau_s)) + M^a \right) \dot{\underline{x}}(T - \tau_s) + a \begin{bmatrix} \sin(T - \tau_s) \\ 0 \\ \vdots \\ 0 \end{bmatrix} \quad (8)$$

where $a = \frac{\alpha}{\omega}$, $b = \frac{\lambda}{\omega}$ and \cdot now refers to differentiation with respect to T .

3. The discrete time overtaking model

The type of system defined by (8) is most commonly solved numerically using the 4th order Runge Kutta (RK4) method; however a naive and computationally faster approach is the Euler Method. For a step size ΔT the Euler method representation of (8) is

$$\underline{v}_{j+1} = \underline{v}_j + \Delta T \left[A^b(\underline{x}_k) + M^a \right] \underline{v}_k + \Delta T a \begin{bmatrix} \sin(\Delta T k) \\ 0 \\ \vdots \\ 0 \end{bmatrix} \quad (9)$$

where v_i is the scaled velocity of the i th vehicle, $v_{ij} = v_i(\Delta T j)$ and $k = j - \frac{\tau_s}{\Delta T}$.

By interpreting Eq. (9) as a model for car following in its own right, we obtain a new model in which the drivers of the following vehicles update their acceleration every ΔT time units and then maintain this constant acceleration for a time period ΔT until their next observation. Thus, in relation to the solution of the car following model (8) the Euler method representation, (9), can be thought of as a discrete time model which involves the repeated application of the well known constant acceleration equation of motion

$$v = u + at \quad (10)$$

where u is the initial velocity, a is the acceleration and v is the velocity after time t .

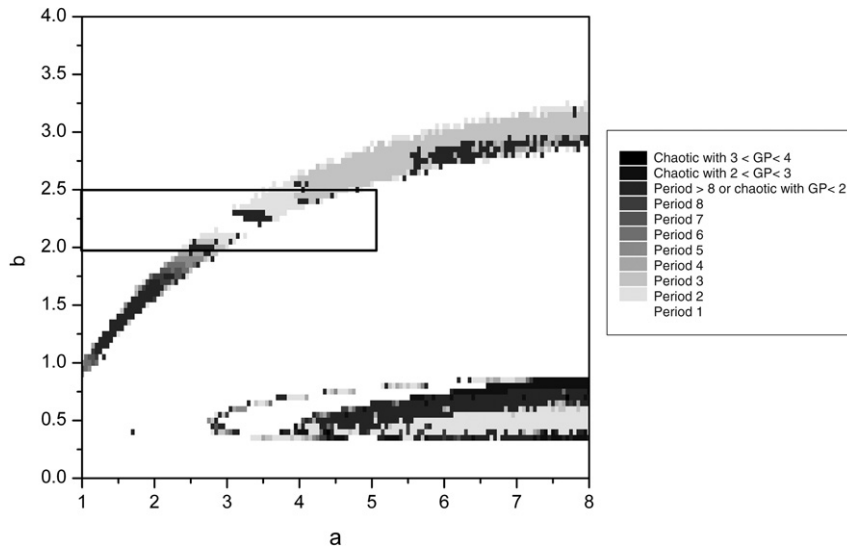


Fig. 1. Periodicity and Grassberger–Procaccia dimension (D_{GP}) plot for the model defined by (8) when the number of vehicles in the system, $n = 3$, the number of points in the reconstructed attractor, $N_p = 3000$, the embedding dimension, $m = 6$, the scaled reaction time of each driver, $\tau_s = 0$ and the scaled length of the ring, $L_s = 0.93$. The physical region of parameter space (equivalent to $0.3 \leq \lambda \leq 0.4$ and $0.15 \leq \alpha \leq 0.8$ in (λ, α) space) is highlighted in black. Note this region also applies to the following corresponding figures.

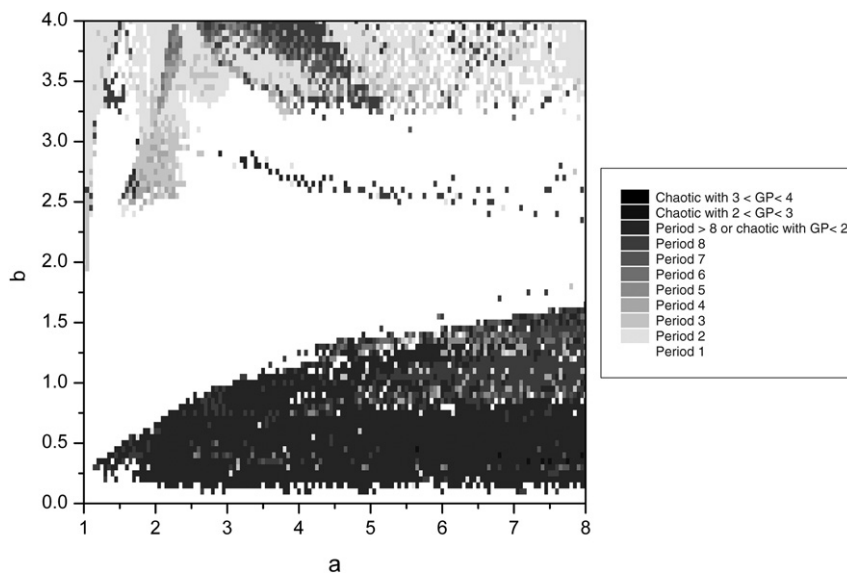


Fig. 2. As for Fig. 1 but with results obtained using the Euler method representation, (9) with $\Delta T = 2\pi/400$ (equivalent to $\Delta t = 0.1$ s).

Perhaps surprisingly, this method of solving a system of time delay differential equations is in fact used in other models of traffic dynamics (see, for example, [16,20]) with ΔT commonly being chosen to be equal to the size of the driver's reaction time, τ_s . The fact that an essentially different model is then being solved is not however explicitly noted in these cases, and although as pointed out by Wilson [21] one expects the dynamics of the model to be affected by the solution method used, this does not appear to be investigated.

In this paper we show that for the overtaking model the method of solution is extremely important and that the results obtained using the Euler method can for some parameter choices be entirely different than those that would be obtained using the more traditional RK4 method. As shown in previous work [18,19] the differential equation based overtaking model defined by (8) can exhibit chaotic behaviour under certain conditions. In this work we analyse the

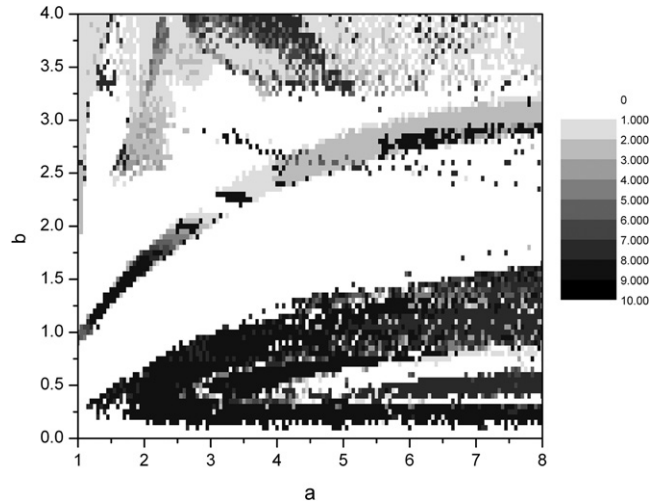


Fig. 3. Absolute difference in category number (where category number is defined as ‘period 1’ = 1, ‘period 2’ = 2 etc. up to ‘chaotic with $3 < D_{GP} < 4' = 11$) between RK4 and Euler method results when $n = 3$, $\tau_s = 0$, $L_s = 0.93$ and $\Delta T = 2\pi/400$ (equivalent to $\Delta t = 0.1$ s).

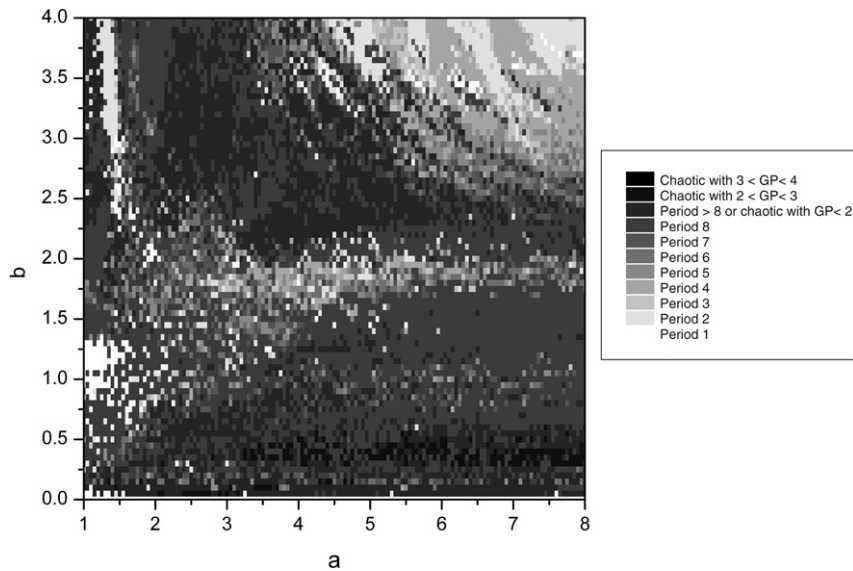


Fig. 4. As for Fig. 1 but with results obtained using the Euler method representation, (9) with $\Delta T = 2\pi/80$ (equivalent to $\Delta t = 0.5$ s).

post-transient behaviour in (a, b) parameter space for both (8) and its difference equation equivalent (9) and measure the percentage of this space in which the post-transient period or fractal dimension, predicted by these models differ for various values of ΔT and τ_s .

4. Parameter space analysis

For our investigations we choose a physically reasonable initial scaled spacing of 0.31 (which is equivalent to 20 m in the case where in the unscaled model, $w_0(t)$ is of the form (7) and $U_0 = 20 \text{ ms}^{-1}$, $A = 0.5$ and $\omega = \frac{2\pi}{40}$) and hence the total scaled length of the ring $L_s = 0.31n$. We restrict our investigations to the case of $n = 3$ vehicles. The parameter space used for our analysis of the model is also chosen to include the physically significant region. This physical region is defined by $0.3 \leq \lambda \leq 0.4$ (equivalent to $2 \leq b \leq 2.5$) and $0.15 \leq \alpha \leq 0.8$ (equivalent to $1 \leq a \leq 5$) in (λ, α) space. The physical limits given here for λ are those found by General Motors in the late

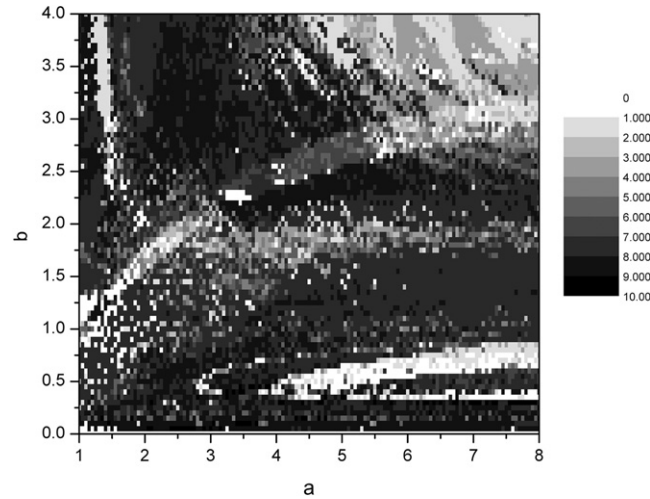


Fig. 5. As for Fig. 3 but with $\Delta T = 2\pi/80$ (equivalent to $\Delta t = 0.5$ s).

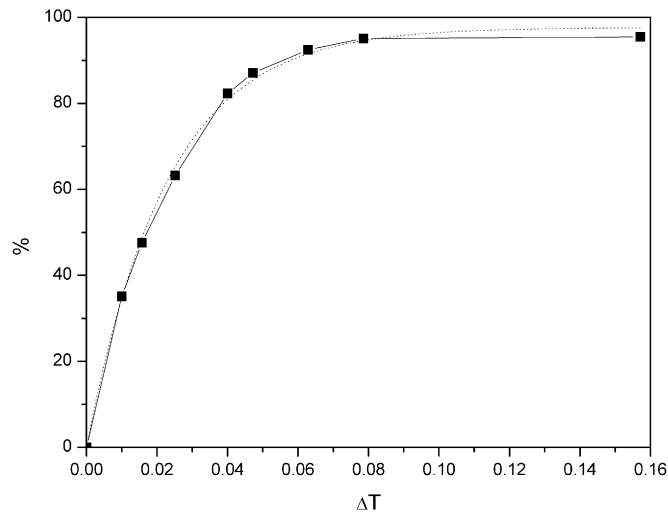


Fig. 6. Percentage of (a, b) space in which the Euler and RK4 methods do not agree for increasing values of ΔT when $n = 3$, $\tau_s = 0$ and $L_s = 0.93$. The (dashed) trend line is of the form (11) with $A = 97.66$, $B = 44$ and the coefficient of determination, $r^2 = 0.998$.

1950s [22] and we choose the limits for α to be defined as above on the assumption that it is physically reasonable for the lead driver's sensitivity to his preferred velocity to lie within the range of the order $\frac{\lambda}{2} \leq \alpha \leq 2\lambda$.

For each point in the (a, b) parameter spaces displayed in the figures below we calculate the period of the post transient oscillations; if this is greater than eight we attempt to distinguish if the attractor simply has a high period or if chaotic behaviour is occurring. To do this we have used the Grassberger–Procaccia dimension algorithm which produces an estimate of the fractal dimension [23,24]. The Grassberger–Procaccia dimension estimate, D_{GP} , is obtained by plotting the logarithm of the correlation integral $C(r)$ against the logarithm of the radius r of a hypersphere placed on the post transient attractor. The slope of the scaling region obtained in this plot is D_{GP} . In each case the attractor is reconstructed from the time series of the scaled velocity of the second vehicle in the stream using 3000 data points and a reconstruction delay time equal to 0.5 scaled time units. The embedding dimension, m , used in each case is equivalent to the dimension of the system being investigated.

The Grassberger–Procaccia dimension distinguishes between regular and chaotic motion as while a D_{GP} value equal to unity indicates that the system is periodic, a value greater than unity indicates that the system has a strange attractor i.e. that the system is chaotic and the larger the D_{GP} value the greater the degree of chaos.

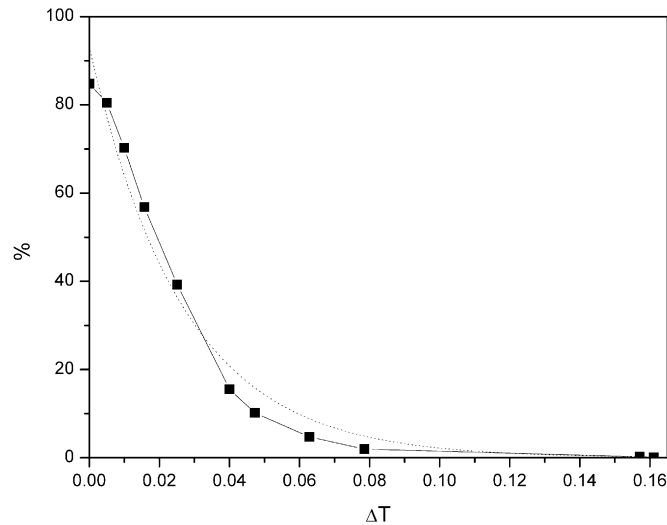


Fig. 7. Percentage of (a, b) space in which the Euler method predicts results which are period 1 for increasing values of ΔT when $n = 3$, $\tau_s = 0$ and $L_s = 0.93$. The (dashed) trend line is of the form $y = Ae^{-Bx}$ with $A = 93.07$, $B = 37.45$ and the coefficient of determination, $r^2 = 0.98$.

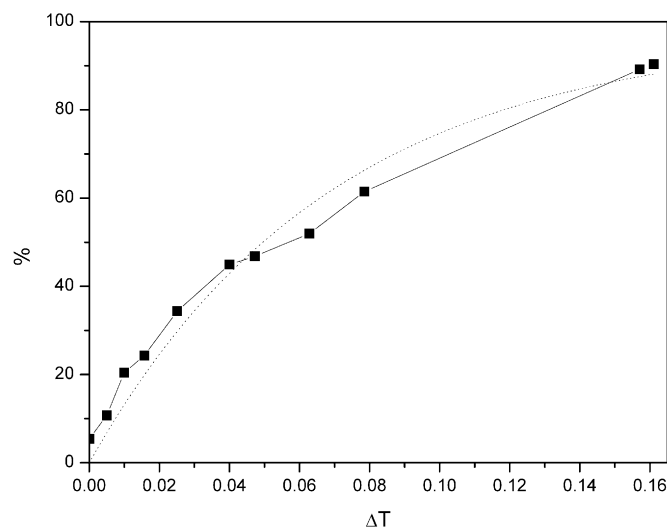


Fig. 8. Percentage of (a, b) space in which the Euler method predicts results which have a period > 8 or are chaotic for increasing values of ΔT when $n = 3$, $\tau_s = 0$ and $L_s = 0.93$. The (dashed) trend line is of the form (11) with $A = 97.53$, $B = 14.51$ and the coefficient of determination, $r^2 = 0.97$.

Fig. 1 shows the results obtained using the RK4 method to solve the differential equation system (8) with $\Delta T = 0.001$ (note that all results calculated using the RK4 method throughout the work presented here use this value of ΔT) and $\tau_s = 0$ and we compare this to the results obtained using the Euler method with various values of ΔT , examples of which are given in Figs. 2 and 4, while the corresponding difference between the two sets of results are shown in Figs. 3 and 5 respectively. This difference is calculated by assigning each point in the parameter space a category number relating to their period ('period 1' = 1, 'period 2' = 2 etc. up to 'chaotic with $3 < D_{GP} < 4$ ' = 11) and then taking the absolute difference between the category number assigned for each of the two solution methods. The % of (a, b) space in which the two methods differ for each value of ΔT examined is shown in Fig. 6. Clearly as ΔT increases the difference in the post-transient results given by the two methods increases rapidly and fitting a trend

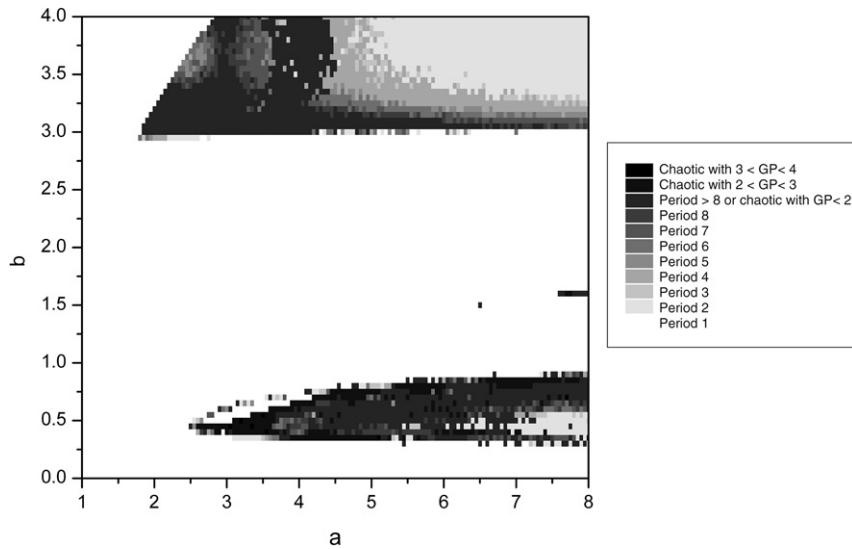


Fig. 9. As for Fig. 1 but with $\tau_s = 2\pi/400$ (equivalent to $\tau = 0.1$ s).

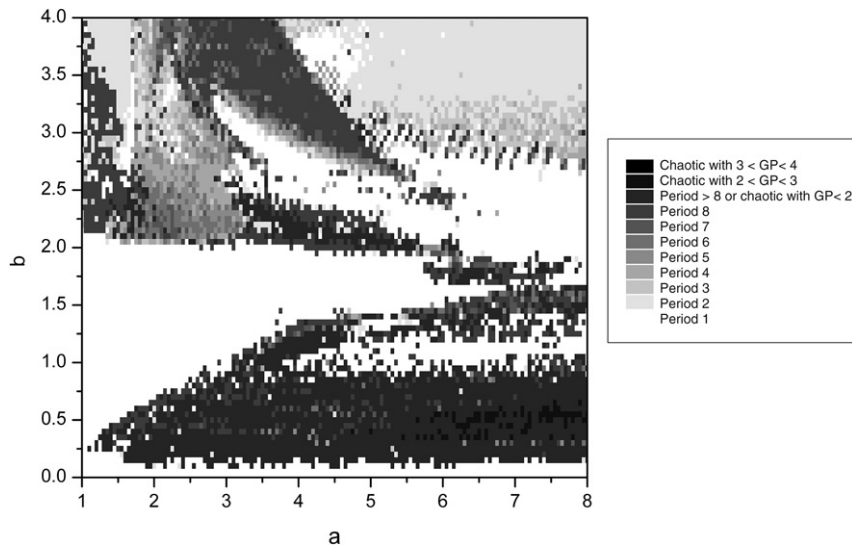
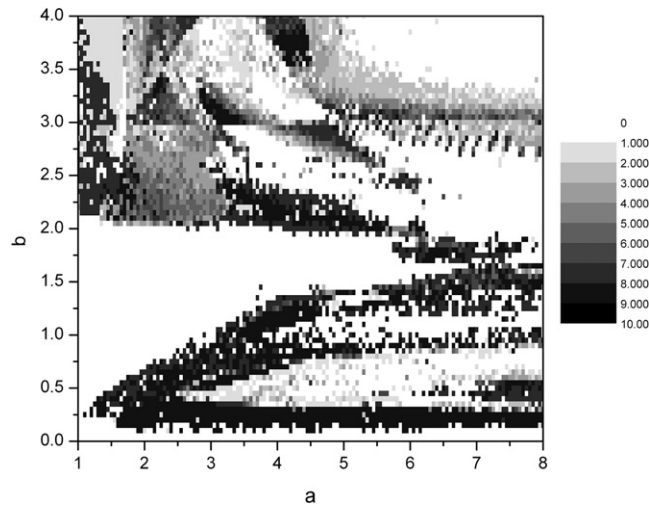
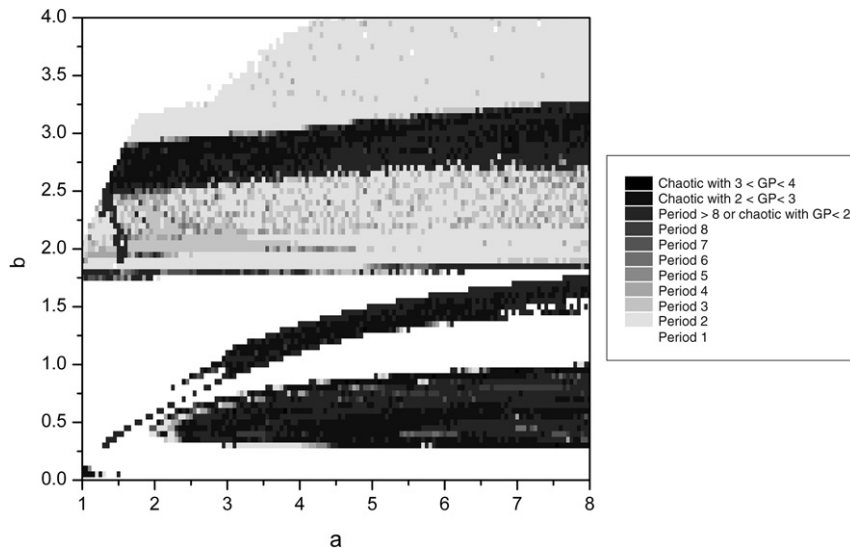


Fig. 10. As for Fig. 1 but with results obtained using the Euler method representation, (9) with $\tau_s = \Delta T = 2\pi/400$ (equivalent to $\tau = \Delta t = 0.1$ s).

line to the data of the form

$$y = A \left(1 - e^{-Bx} \right), \quad (11)$$

gives good agreement and indicates the rapidity of growth in the difference between the results predicted by the two models. Note from Fig. 6 that the discrete and continuous models disagree with regard to the post transient period or Grassberger–Procaccia dimension in nearly 50% of the (a, b) parameter space considered when $\Delta T = 0.02$ and this rises to over 90% when $\Delta T = 0.1$. Interestingly, comparing Figs. 1 and 2 we find that in the physically significant region the discrete time model with $\Delta T = 2\pi/400$ is more stable in that it exhibits less period inflation and no chaotic behaviour in comparison to the equivalent continuous time model. Clearly this is not the case for the wider region of parameter space shown in Figs. 1 and 2, but nonetheless it should be noted that such a result may deceive the unwary into believing that the solution method is of limited importance.

Fig. 11. As for Fig. 3 but with $\tau_s = \Delta T = 2\pi/400$.Fig. 12. As for Fig. 1 but with $\tau_s = 2\pi/80$ (equivalent to $\tau = 0.5$ s).

Significantly, as is shown in Figs. 7 and 8, as ΔT increases in the discrete time model the percentage of (a, b) parameter space which has a period 1 attractor decreases, while that which has an attractor of period > 8 or a chaotic attractor increases. This indicates that as ΔT increases the type of results obtained by each method become increasingly different and therefore any results obtained using the discrete time model will be unrepresentative of how traffic modelled by the original continuous time model behaves.

As mentioned above, in discrete time simulation models the size of the driver's reaction time is more commonly taken to be equal to the size of the time step, ΔT , and therefore we again investigate the difference between the RK4 and Euler methods for values of $\tau_s > 0$. This is shown in the sequence of Figs. 9–15. In Figs. 9–11 $\tau_s = 2\pi/400$ (equivalent to $\tau = 0.1$ s). Comparing Fig. 3 with Fig. 11 we note that introducing time delay into the systems, while not greatly effecting the total percentage of (a, b) space in which the differential (8) and difference (9) equation models differ, causes the regions in which a difference exists to shift more into the physically significant region $1 \leq a \leq 5$ and $2 \leq b \leq 2.5$. As before we find that increasing ΔT , and hence in this case τ_s , leads to the difference in the behaviour resulting from each model to grow and this growth approximately fits a function of the form (11).

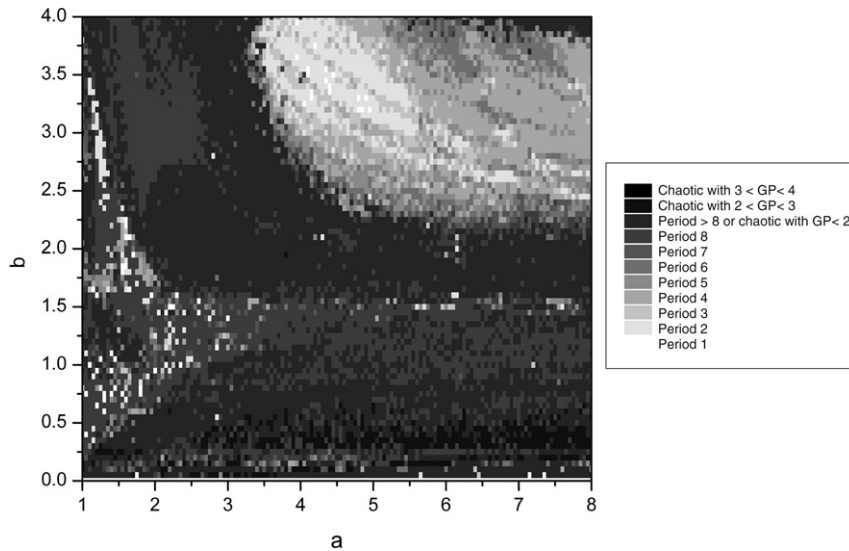


Fig. 13. As for Fig. 1 but with results obtained using the Euler method representation, (9) with $\tau_s = \Delta T = 2\pi/80$ (equivalent to $\tau = \Delta t = 0.5$ s).

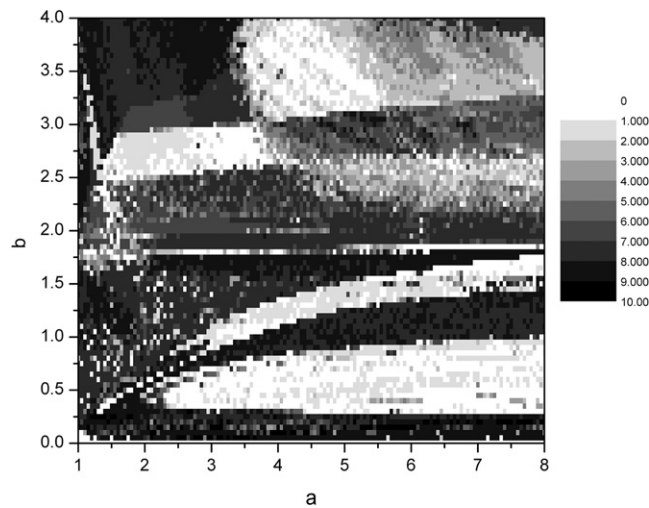


Fig. 14. As for Fig. 3 but with $\tau_s = \Delta T = 2\pi/80$.

5. Conclusion

In this paper we have investigated the effect of discretizing a car following model in which the real traffic phenomenon of vehicle passing is permitted. Analysis of the resulting behaviour and comparison with the continuous form of the model shows that the discretization can for certain parameter values dramatically affect the type of post-transient behaviour exhibited by the system. For both the continuous and discrete forms of the model, within physically meaningful regions of parameter space the corresponding system can exhibit a wide variety of behaviour including both periodic and chaotic behaviour resulting from a periodic perturbation. Significantly as the size of the time step used in the discrete time model is increased the percentage of parameter space in which the system is chaotic increases rapidly. Thus for example a (scaled) time step-size in the discrete model of $\Delta T = 0.02$ results in the periodicity of the post transient behaviour in the discrete time model and continuous model being different in approximately 50% of the (a, b) parameter space considered, and this rises to over 90% when $\Delta T = 0.1$.

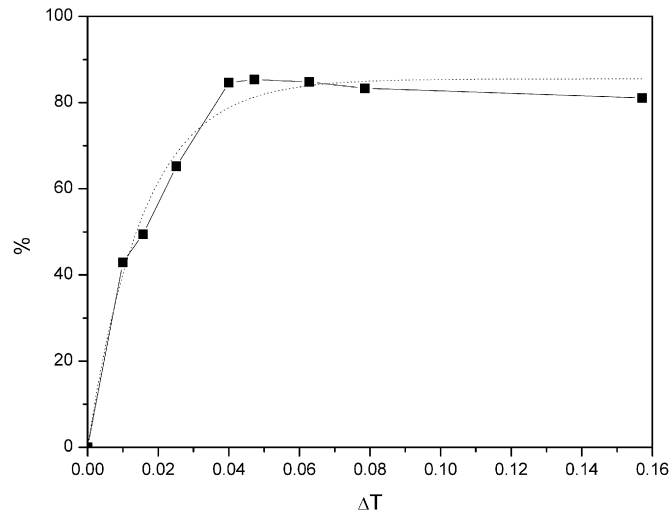


Fig. 15. Percentage of (a, b) space in which the Euler and RK4 methods do not agree for increasing values of ΔT when $n = 3$, $\tau_s = \Delta T$ and $L_s = 0.93$. The (dashed) trend line is of the form (11) with $A = 85.49$, $B = 63.71$ and the coefficient of determination, $r^2 = 0.98$.

The work described here shows that for the overtaking model the method of solution is therefore extremely important, and that if solving the system in discrete time it is necessary to note that the dynamics of the model are then changed and hence the results obtained may not be representative of those that would be obtained using the continuous time model.

Finally, we note that not only does the difference in solution methods yield different results, but just as importantly in a modelling context the different solution methods represent different mathematical models of the process being considered. Thus one should not necessarily assume that the model based on differential equation (8) is a better model (in the sense that it more accurately describes the reality being modelled) than that based on the difference equation (9). Indeed it has been argued elsewhere [25,26] that a model incorporating discontinuous updates in behaviour may reflect more accurately actual driver behaviour.

References

- [1] M. Brackstone, M. McDonald, Car following: A historical review, *Transportation Research Part F: Traffic Psychology and Behaviour* 2 (2000) 181–196.
- [2] D.C. Gazis, *Traffic Theory*, Kluwer Academic Publishers, 2002.
- [3] M. Bando, K. Hasebe, A. Nakayama, A. Shibata, Y. Sugiyama, Dynamical model of traffic congestion and numerical simulation, *Physical Review E* 51 (1995) 1035–1042.
- [4] M. Bando, K. Hasebe, K. Nakanishi, A. Nakayama, Analysis of optimal velocity model with explicit delay, *Physical Review E* 58 (1998) 5429–5435.
- [5] R.E. Wilson, P. Berg, S. Hooper, G. Lunt, Many neighbour interactions and non-locality in traffic models, *European Physics Journal B* 39 (2004) 397–408.
- [6] L.C. Davis, Modifications of the optimal velocity model to include delay due to driver reaction time, *Physica A* 319 (2003) 557–567.
- [7] G. Orosz, R.E. Wilson, B. Krauskopf, Global bifurcation investigation of an optimal velocity model with driver reaction time, *Physical Review E* 70 (2004) 026207.
- [8] M. McCartney, A trip time model for traffic flow on a semi-closed loop, *Transportation Research B* (2005) (submitted for publication).
- [9] S. Jamison, M. McCartney, Investigating a class of car following model on a ring, in: B. Hydecker (Ed.), *Proceedings of Forth IMA Conference on Mathematics in Transport*, Elsevier, 2007, pp. 97–110.
- [10] M. McCartney, S. Gibson, Differential equations, traffic dynamics and the N roots of unity, *The Mathematical Gazette* 90 (2006) 502–505.
- [11] M. McCartney, S. Gibson, The routes of unity, *International Journal of Mathematical Education in Science and Technology* 37 (2006) 992–998.
- [12] D.C. Gazis, R. Herman, R.W. Rothery, Nonlinear follow the leader models of traffic flow, *Operations Research* 9 (1961) 545–567.
- [13] D. Jarrett, Z. Xiaoyan, The dynamic behaviour of road traffic flow: Stability or chaos? in: A.J. Crilly, R.A. Earnshaw, H. Jones (Eds.), *Applications of Fractals and Chaos*, Springer-Verlag, Berlin, Heidelberg, New York, 1993.
- [14] P.S. Addison, D.J. Low, A novel nonlinear car-following model, *Chaos* 8 (1998) 791–799.
- [15] D.J. Low, P.S. Addison, A nonlinear temporal headway model of traffic dynamics, *Nonlinear Dynamics* 16 (1998) 127–151.

- [16] P.G. Gipps, A behavioural car following model for computer simulation, *Transportation Research B* 15 (1981) 105–111.
- [17] SISTM, A motorway simulation model, Leaflet LF2061, Transportation Research Laboratory, 1993.
- [18] S. Jamison, M. McCartney, A velocity matching car following model on a closed ring in which overtaking is allowed, *Nonlinear Dynamics* (2006) (submitted for publication).
- [19] S. Jamison, M. McCartney, A vehicle overtaking model of traffic dynamics, *Chaos* 17 (2007) 033116.
- [20] J. Wang, F. Montgomery, Car following model for motorway traffic, *Transportation Research Record* 1934 (2005) 33–42.
- [21] R.E. Wilson, An analysis of Gipps's car following model of highway traffic, *IMA Journal of Applied Mathematics* 66 (2001) 509–537.
- [22] F.E. Chandler, R. Herman, E.W. Montroll, Traffic dynamics: Studies in car following, *Operations Research* 6 (1958) 165–184.
- [23] P. Grassberger, I. Procaccia, Characterisation of strange attractors, *Physical Review Letters* 50 (1983) 346–349.
- [24] P. Grassberger, I. Procaccia, Measuring the strangeness of strange attractors, *Physica D* 9 (1983) 189–208.
- [25] M. McCartney, A discrete time car following model & the bi-parameter logistic map, *Communications in Nonlinear Science and Numerical Simulation* (2007) (in press).
- [26] M. McCartney, Inattentive drivers: Making the solution method the model, *International Journal of Mathematical Education in Science and Technology* 34 (2003) 609–621.